INL/CON-11-21340
PREPRINT

Effects of Graphite Surface Roughness on Bypass Flow Computations for an HTGR

ASME 2011 Pressure Vessels and Piping Division Conference

Yu-Hsin Tung
Richard W. Johnson
Hiroyuki Sato

July 2011

The INL is a
U.S. Department of Energy
National Laboratory
operated by
Battelle Energy Alliance

Proceedings of the ASME 2011 Pressure Vessels and Piping Division Conference
PVP2011
July 17-21, 2011, Baltimore, Maryland

PVP2011-58053

EFFECTS OF GRAPHITE SURFACE ROUGHNESS ON BYPASS FLOW COMPUTATIONS FOR AN HTGR

Yu-Hsin Tung
INL Intern
National Tsing Hua University
Hsinchu,Taiwan
Yu-Hsin.Tung@inl.gov

Richard W. Johnson
Idaho National Laboratory
Idaho Falls, Idaho, USA
Rich.Johnson@inl.gov

Hiroyuki Sato
Japan Atomic Energy Agency
Oarai, Ibaraki, Japan
sato.hiroyuki09@jaea.go.jp

ABSTRACT

Bypass flow in a prismatic high temperature gas reactor (HTGR) occurs between graphite blocks as they sit side by side in the core. Bypass flow is not intentionally designed to occur in the reactor, but is present because of tolerances in manufacture, imperfect installation and expansion and shrinkage of the blocks from heating and irradiation. It is desired to increase the knowledge of the effects of such flow; it has been suggested that it may be 20% of the total helium coolant flow [INL report 2007, INL/EXT-07-13289]. Computational fluid dynamic (CFD) simulations can provide estimates of the scale and impacts of bypass flow. Previous CFD calculations have examined the effects of bypass gap width, level and distribution of heat generation and effects of shrinkage. The present contribution examines the effects of graphite surface roughness on the bypass flow for different relative roughness factors on three gap widths. Such calculations should be validated using specific bypass flow measurements. While such experiments are currently underway for the specific reference prismatic HTGR design for the next generation nuclear plant (NGNP) program of the U.S. Dept. of Energy, the data are not yet available. To enhance confidence in the present calculations, wall shear stress and heat transfer results for several turbulence models and their associated wall treatments are first compared for flow in a single tube that is representative of a coolant channel in the prismatic HTGR core. The results are compared to published correlations for wall shear stress and Nusselt number in turbulent pipe flow. Turbulence models that perform well are then used to make bypass flow calculations in a symmetric one-twelfth sector of a prismatic block that includes bypass flow. The comparison of shear stress and Nusselt number results with published correlations constitutes a partial validation of the CFD model. Calculations are also compared to ones made previously using a different CFD code. Results indicate that increasing surface roughness increases the maximum fuel and helium temperatures as do increases in gap width. However, maximum coolant temperature variation due to increased gap width is not changed by surface roughness.

INTRODUCTION

The core of the reference prismatic version of the HTGR consists of stacks of hexagonal blocks of graphite drilled to accept cylindrical fuel compacts and to provide for coolant flow. Figure 1 illustrates the cross section of one such block. The smaller blue circles represent fuel elements while the red circles represent coolant channels. Gaps occur between adjacent hexagonal blocks where the coolant can flow, bypassing the coolant channels. Figure 1 also illustrates the location of a one-twelfth sector that is symmetric along each edge, one of which is a bypass flow gap. The CFD model used in the present calculations is based on the symmetric one-twelfth sector, which is extruded through the entire core.

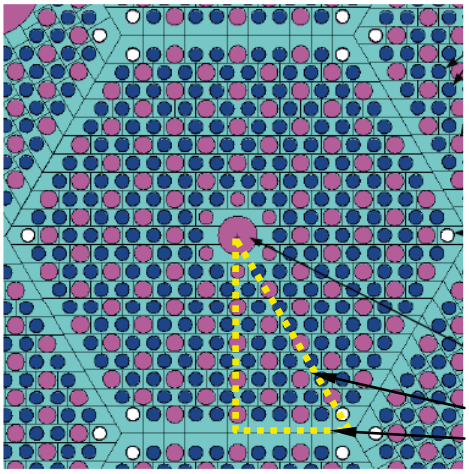

Fig. 1. Graphite block and symmetric 1/12 sector.

The reference prismatic HTGR is based on the General Atomics modular high temperature gas reactor (MHTGR) [1], which generates a nominal 350 MW_{th}.power. The prismatic core consists of nine rings of graphite blocks, 66 of which contain fuel and coolant channels. Figure 2 illustrates the cross section of the prismatic core with the heated blocks shown in lighter blue. Dark blue graphite blocks are reflector blocks. There are also reflectors at the top and the bottom of the core. Blocks are 0.793 meters in height; there are ten heated blocks in each stack. Helium flows upwards in ducts around the outside of the outer reflector into an upper plenum and then downwards through the core into the lower plenum where it exits through a hot duct. The hot duct is annular with cooled helium returning to the reactor vessel through the annulus.

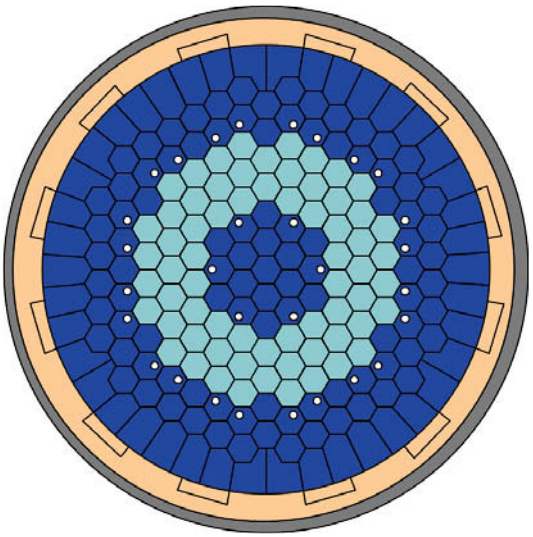

Fig. 2. Plan view of the prismatic core barrel.

Several computational studies have been made to estimate detailed flow and temperature distributions for flow in a prismatic reactor using a symmetric one-twelfth sector extruded through the reactor core. Tak et al. [2] report flow and temperature distributions from CFD calculations for a prismatic core with a nominal 1000°C outlet coolant temperature. However, they used a separate 1D code to provide flow rate information for their CFD calculations. Sato et al. [3] produced CFD calculations for a nominal 600 MW_{th} very high temperature reactor (VHTR) for different gap widths. In their calculations, they used stagnation pressure inlet and pressure outlet boundary conditions such that the flow rates were determined as a result of the simulations. Also, they assumed that the pressure drop was the same for all bypass gap widths, such that the bypass flow was not 'robbed' from the coolant channel flow. In a later publication, for the same nominal 600 MW_{th} VHTR, Sato et al. [4] computed bypass flow for different gap widths for the case where the bypass flow is 'robbed' from the coolant channel flow. They lowered the pressure drop for larger gap widths such that the total flow rates remained the same for all gap width cases. They also computed the effects of using different turbulence models, uniform versus axially varying heat generation rates and the effects of shrinkage.

As the reference design was modified to be a 350 MW_{th} HTGR, additional calculations were reported by Johnson and Sato [5] for different gap widths using the same total mass flow rate, uniform versus axially varying heat generation rates and block shrinkage. These calculations show that the hottest fuel compact and coolant temperatures increase as bypass flow gap width increases where the bypass flow is 'robbed' from the coolant channels. Further, they show that the variation in outlet coolant temperature increases dramatically from the reference case of zero gap width. This finding has significant implications about the helium temperature in the lower plenum. It is desired that the helium be thermally well mixed by the time it exits through the hot duct so that it doesn't have a deleterious effect on downstream equipment such as electrical generating turbines or intermediate heat exchangers.

The objective of the present study is to estimate the effects of graphite surface roughness on the bypass flow in the one-twelfth sector for the nominal 350 MW_{th} HTGR based on the General Atomics MHTGR.

CFD MODEL

The CFD model is based on a one-twelfth sector of a prismatic core block, as indicated in Fig. 1, which has symmetric edges on all sides. The model includes a 1.189m graphite upper reflector and a 1.585m lower reflector [1]. The center 7.93 m contains heated fuel compacts. The fuel compacts are assumed to run from the top of each block to the bottom. The coolant channels run through the length of the model. Only one-half of the gap is included in the model because of symmetry. The fuel compacts have a diameter of 12.70mm. Most coolant channels have a diameter of 15.88mm; the coolant channel closest to the center is 12.70mm dia. Figure 3 shows a cross sectional view of the CFD model with locations of the bypass flow gap and fuel and coolant channels. Symmetry boundaries are used along all three surfaces represented by the edges in Fig. 3. The block handling hole is ignored in the CFD model and set to graphite properties. The 7.6 million cell mesh was generated using GAMBIT 2.4.6 [6].

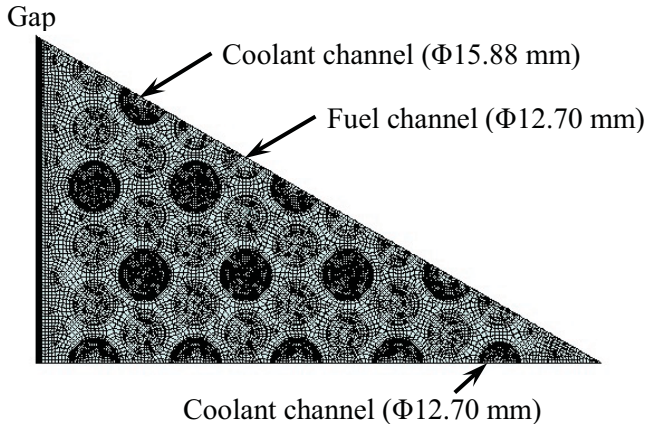

Fig. 3 Cross sectional view of the CFD model with mesh.

The channel and gap inlets are set to stagnation pressure inlets; the outlets are set to pressure outlets. The flow is induced by setting a pressure difference between the inlets and outlets. Thermal and transport properties for the helium are obtained from the National Institute of Standards and Technology (NIST) of the U. S. Dept. of Commerce [7]; the properties are for 6.4 MPa and are assumed to be isobaric. The graphite properties are taken from a General Atomics graphite report [8]. The fuel compact properties are those used in an earlier study by the INL [9]. The inlet temperature for the gap and coolant channels is set to 532K (259°C). The heat generation profile for the one-twelfth sector computations is based on a 'cosine' varying profile. Equation (1) is used in the CFD code to specify the heat generation rate as a function of the core depth coordinate z:

$$q''' = A_r q_{con} \left\{ 1 + \left(A_p - 1 \right) \sin \left[\frac{\pi (z - 1.189)}{L} \right] \right\} \qquad (1)$$

where A_r is the radial factor, A_p is the peak axial factor given as 1.3, L is the length of the heated section (7.93m), 1.189 is thickness of the upper reflector and q_{con} is a constant that is tuned to provide the total heat generation desired in the core. q_{con} is set to 21,103,716 W/m^3 for the 350 MW$_{th}$ HTGR being considered. The peak radial factor, given as 1.25 [9], is the expected maximum factor by which the heat generation rate will exceed the average heat generation rate in the radial (lateral) coordinate in the core. Figure 4 plots the heat generation rate for the average and the peak radial factors.

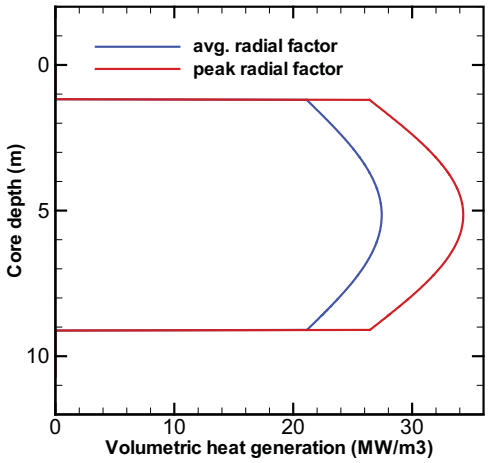

Fig. 4. Peak and average heat generation rates.

BEST PRACTICES

The guidelines developed by the Fluids Engineering Division of ASME for publication of numerical calculations in their journal [10] were followed for the present simulations. The commercial CFD code STARCCM+ [11] is used for the present calculations, except where noted. The discretization is formally second order accurate. Iterative convergence was investigated by computing laminar fully developed flow in a tube and comparing with the analytical solution. It was found that a residual tolerance of 1 x 10^{-4} using STARCCM+ was sufficient for iterative convergence. All results reported herein for STARCCM+ are converged to 1 x 10^{-6}. Grid convergence was demonstrated for the present grid in an earlier study [4]. There, a refined grid of 10.9 million cells was used to obtain comparative results. The maximum temperature for the fuel was within 0.35% of the value from the coarser grid. Finally, validation exercises have been conducted that partially validate the present calculations. Full validation awaits the completion of validation experiments as mentioned earlier. The validation exercises are presented in the next section.

VALIDATION EXERCISES

Validation exercises are performed for helium flow in a single coolant channel. The single coolant channel has the same length as the actual core, described above. A representative heat flux is used to heat the coolant as it passes through the heated section of the single coolant channel. Because the temperature of the helium increases as it flows through the tube, its viscosity increases and, hence, the flow Reynolds number decreases. This means that the wall shear stress and Nusselt number are functions of core depth for the exercises performed. Correlations for friction factor and Nusselt number depend on Reynolds and Prandtl numbers. In order to apply the correlations, the Reynolds number has to be calculated for the flow as a function of core depth. This is accomplished by computing the heat input into the helium and thereby computing the bulk temperature as a function of core depth. The properties of the helium at the bulk temperature are then used to compute the Reynolds number.

Wall Shear Stress

The wall shear stress is computed for a number of turbulence models that are available in STARCCM+ [11] for smooth tubes. In addition to applying the turbulence model, a wall treatment must also be applied. The wall treatment deals with the turbulence quantities in the region adjacent to the wall. Of course, the wall treatment is very important to the prediction of wall shear stress as well as heat transfer coefficient. In the validation exercises reported below, the all y^+ wall treatment is used for every case, where y^+ is the dimensionless distance from the wall adjacent node to the wall. In a typical turbulent boundary layer, the flow adjacent to the wall is nonturbulent or laminar. Further out, the flow is turbulent and has a logarithmic velocity profile. In between, there is a transition or buffer layer. The laminar sublayer is typically within a y^+ value of about 11. The log-law region is typically valid for $30 < y^+ < 300$ [6]. The all y^+ wall treatment is designed to be able to handle near-wall nodes that are in the laminar sublayer, the buffer layer or the turbulent log-law layer [11]. The code manual [11] further indicates that the all y^+ wall treatment is customized for each particular turbulence model. Results for two different grids are reported. While y^+ varies along the coolant tube because of the change in wall shear stress, the dimensional wall-adjacent mesh cell is constant in width. A medium grid is used with a range of y^+ values of from 6 to 12. A finer grid is also employed where

the range of y^+ values is from 1.7 to 2.6. Both of these ranges are nominally within the laminar sublayer on average. The turbulence models employed include:

- Standard k~ε two layer model
- Standard k~ε low Re model
- Realizable k~ε two layer model
- Abe-Kondoh-Nagano low Re model
- Standard (Wilcox) k~ω model
- Shear stress transport (SST) (Menter) k~ω model
- Reynolds stress two layer model
- Standard Spalart-Allmaras model

The two layer modeling approach [11] of some of the above models divides the flow domain into a near wall layer and the rest of the domain. In the near wall layer, the dissipation rate (ε) and turbulent viscosity are computed from empirically obtained functions. The dissipation rate is blended with that computed from the differential model equation in the outer flow. The turbulent kinetic energy (k) is computed from the model equation throughout both layers. Note that the two-layer approach is not the same as the wall function approach. The low Reynolds number turbulence models employ damping functions applied to some of the modeling coefficients that appear in the turbulence models for the various turbulence quantities. Details can be found in the code manual [11].

Published correlations for wall shear stress (friction factor) used to compare with the present results include the following:

$$\frac{1}{\sqrt{f}} = 2\log\left(\mathrm{Re}\sqrt{f} - 0.8\right) \text{ (Prandtl) [12]} \quad (2)$$

$$f = 0.3164\mathrm{Re}^{-0.25} \text{ (Blasius) [13]} \quad (3)$$

$$\frac{1}{\sqrt{f}} = -2.0\log\left(\frac{e/D}{3.7} + \frac{2.51}{\mathrm{Re}\sqrt{f}}\right) \text{ (Colebrook) [13]} \quad (4)$$

$$f = 0.0014 + 0.125\mathrm{Re}^{-0.32} \text{ (Drew et al.) [14]} \quad (5)$$

Figure 5 plots the wall shear stress computed using the standard k~ε two layer turbulence model with the all y^+ wall treatment for the case of the fine grid (y^+ from 1.7 to 2.6) compared to the four correlations. The maximum variations in the CFD predictions from the correlations range from 4.5 to 6.1%. Figure 6 plots the wall shear stress for the realizable k~ε two layer turbulence model for the same grid. Maximum variations range from 1.2 – 2.7%. Figure 7 plots the wall shear stress for the shear stress transport (SST) (Menter) k~ω turbulence model, also for the fine grid. Maximum variations range from 13.4 – 14.6%. Table 1 provides a summary of the maximum variations for the shear stress validation exercise.

It seems reasonable that shear stress results that are within 5-6% of the published correlations are adequate to accurately represent the friction occurring in the coolant channels. From Table 1, it is seen that all but the standard k~ε low Re and the two k~ω models accomplish this for the fine grid, though the AKN low Re model is borderline. For the medium grid, it is seen that the standard k~ε two layer, the AKN low Re and the standard Spalart-Allmaras turbulent models are acceptable.

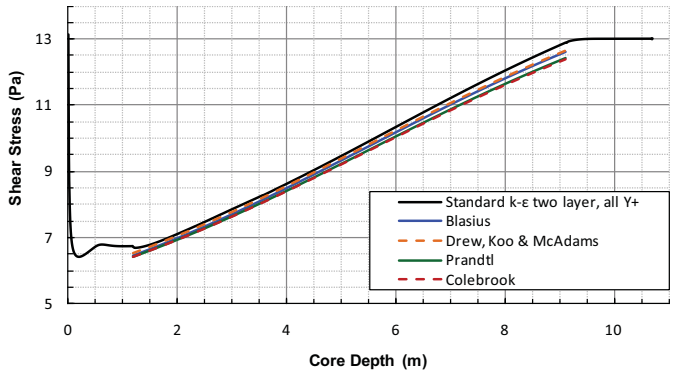

Fig. 5. Shear stress for the standard k~ε two layer model.

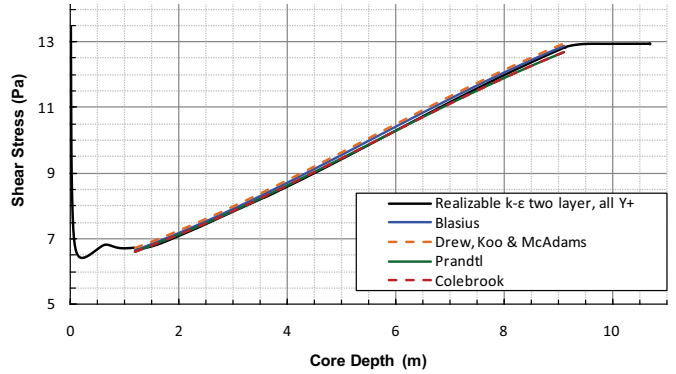

Fig. 6. Shear stress for realizable k~ε two layer model.

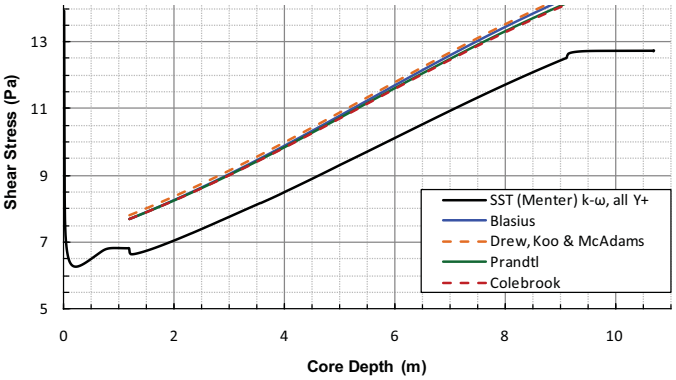

Fig. 7. Shear stress for the SST (Menter) k~ω model.

Table 1. Maximum variations (%) of shear stress for 8 turbulence models relative to 4 friction correlations.

Mesh	SKE 2 lay	SKE low Re	RKE 2 lay	AKN low Re	SKΩ	SST	RSM 2 lay	SSA
med.	4.6-6.0	25.0-27.7	10.4-11.7	4.7-6.1	26.9-29.7	25.8-28.6	10.4-11.9	3.7-5.2
fine	4.5-6.1	6.1-7.7	1.2-2.7	5.4-6.7	12.9-14.2	13.4-14.6	1.1-2.6	2.1-3.6

Nusselt Number

Based on the results for the fine grid on the prediction of wall shear stress, an additional exercise to compute the Nusselt number and compare it to a published correlation was performed. For this exercise, the following turbulence models (all with the all y^+ wall treatment) were employed:

- Standard k~ε two layer model
- Realizable k~ε two layer model
- Reynolds stress two layer model
- Standard Spalart-Allmaras model

The correlation for Nusselt number for flow in smooth tubes (which may or may not produce correct values for rough tubes) used for comparison is from McEligot et al. [15] and is applicable to gas flow with varying fluid properties due to temperature variation:

$$\mathrm{Nu} = 0.021\mathrm{Re}^{0.8}\mathrm{Pr}^{0.4}(T_w/T_b)^{-0.5} \qquad (6)$$

The Reynolds number, the Prandtl number and the temperature ratio that appear in Eqn. (6) all vary with core depth and are calculated separately from the CFD code based on the variation of wall and bulk temperature computed by the CFD code. Figure 8 plots the Nusselt number versus core depth for the standard k~ε two layer model for the fine grid and compares the results to the correlation results. The minimum to maximum deviation from the correlation (6) is from 6.7 to 8.3%, which seems somewhat high. Note that the range of y^+ is the same as reported earlier for the wall shear stress exercises (1.7 – 2.6). Figure 9 plots the Nusselt number versus depth for the realizable k~ε two layer model for the fine grid. For this case the minimum to maximum variation is from 3.7 to 4.9%, which is very reasonable. Table 2 tabulates the results for the four turbulence models for the two grids. It can be seen from Tables 1 and 2 that the realizable k~ε two layer model using the all y^+ wall treatment yields satisfactory results for both the wall shear stress and the heat transfer coefficient for the fine grid. The range of y^+ for the one-twelfth sector CFD model that is used for the bypass flow calculations is below a value of 6.

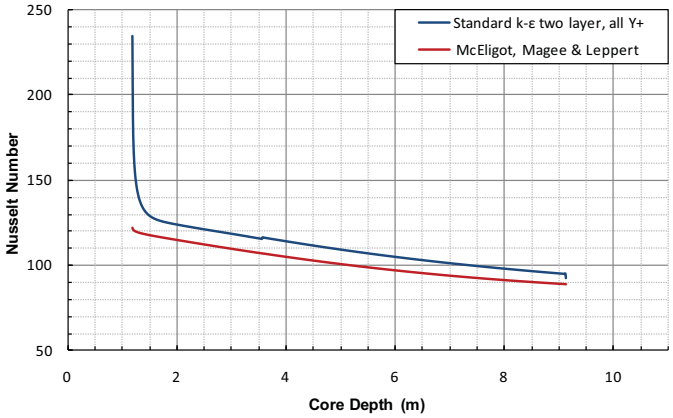

Fig. 8. Nusselt number for standard k~ε two layer model.

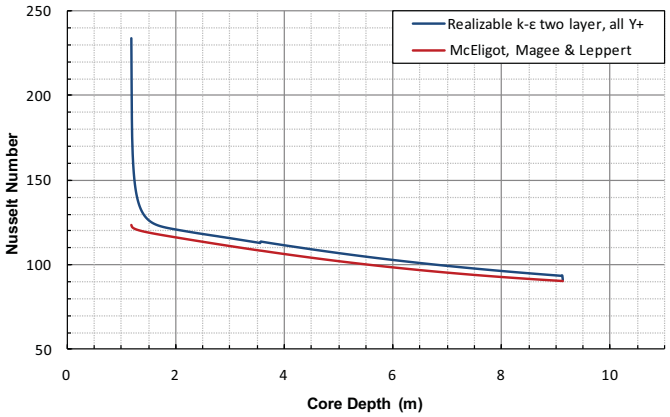

Fig. 9. Nusselt number for realizable k~ε two layer model.

Table 2. Minimum to maximum variations (%) from Nusselt number correlation of McEligot et al. [15].

Mesh	SKE 2 lay	RKE 2 lay	RSM 2 lay	SSA
medium	4.1-8.3	0.004-3.0	5.9-7.9	4.4-7.5
fine	6.7-8.3	3.7-4.9	0.001-1.1	5.3-7.7

Wall Shear Stress for Rough Graphite Surfaces

Warburton [16] made roughness and friction factor measurements on eight graphite tubes machined to have from a smooth surface up to the roughest surface expected to occur in an Advanced-Gas-Cooled-Reactor in Great Britain. He used two techniques to assess the surface roughness. From traces provided in the article, it is obvious that the roughness 'elements' are not uniform like some roughness tests made by other researchers, e.g. Nikuradse [17]. However, the range of roughness elements provides some information on possible roughness that might be expected in the HTGR. Two averaged roughness heights are taken from Warburton [16], including the roughest surface and a mid-range surface for purposes of including surface roughness in the CFD simulation for bypass flow in the one-twelfth sector of the HTGR. The roughness is measured in Ref. [17] by performing an average of peak to valley measurements over smaller intervals and dividing by the tube diameter. The two roughness elements chosen have dimensional values of 1.586×10^{-5} and 2.509×10^{-5} m. Dividing by the diameter of the most common coolant channel size (15.88 mm), relative roughness values of 1.0×10^{-3} and 1.57×10^{-3} are obtained. Results using the realizable k~ε two layer turbulence model and the all y+ wall treatment along with the roughness model are plotted in Fig. 10 and compared to the curves generated using the Colebrook correlation, Eqn. (4), which includes a relative roughness term (e/D). The minimum and maximum variations are from 0.001 to 0.41% for relative roughness of 1.0×10^{-3} and 2.58 to 4.96% for 1.57×10^{-3} (ignoring the peaks at the end of the curve, which are within the upper reflector). It should be noted that the shear stress values measured by Warburton [17] for relative roughness of 1.0×10^{-3} match the Colebrook correlation very well; the Colebrook values for the higher roughness factor of 1.58×10^{-3} are on the

order of 20% below the shear stress he measured. Inasmuch as the present paper is simply performing parametric studies of surface roughness, this discrepancy is not of significant concern. When new data are taken regarding relative roughness of the graphite expected to be used in the HTGR, new calculations can be made.

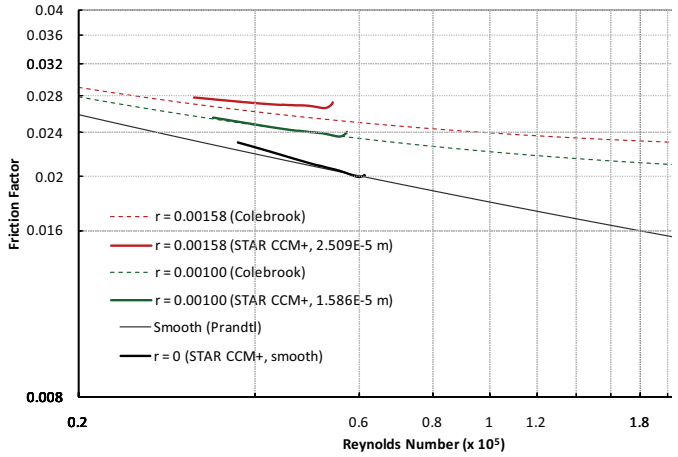

Fig. 10. Friction factor for CFD results vs. Colebrook.

RESULTS AND DISCUSSION

CFD computations are made for the one-twelfth symmetric sector of a prismatic core block through the whole core as described earlier. Variations in flow and temperature values are compared for FLUENT versus STARCCM+ for similar turbulence models, standard versus realizable k~ε two layer turbulence models in STARCCM+ and finally for smooth versus rough graphite wall for two roughness factors.

Comparison of CFD Codes

As discussed above, previous results for CFD simulations for flow in a one-twelfth sector for variations in gap width, heat generation profile, block shrinkage and total reactor power reported in Refs. [3, 4, 5] were performed using commercial CFD code FLUENT [6]. The standard k~ε turbulence model using the enhanced wall treatment was employed. The enhanced wall treatment in FLUENT is based on the same philosophy as the all y^+ wall treatment in STARCCM+. That is, it is designed to accommodate the grid employed whether the near wall node is in the laminar sublayer, the transition layer or the turbulent log-law layer. Calculations are made for a 3mm bypass gap for the same pressure drop using both FLUENT and STARCCM+; the standard k~ε turbulence model with all y^+ wall treatment is used in the latter. The axially varying heat generation at the peak radial factor is used. Figure 11 provides values of bulk outlet temperatures and mass flow rates for the two simulations. (Note that mass flows in the figures are all for whole channels.) It can be seen that the outlet temperatures for STARCCM+ are slightly lower than for FLUENT with the mass flow rates correspondingly slightly higher. The two results compare very well. Table 3 provides comparisons of important input and output information including sector-only helium flow rate, gap flow fraction, maximum fuel temperature, gap outlet temperature, maximum outlet coolant temperature and the maximum variation in outlet helium temperature. Differences are due mostly to turbulence model differences.

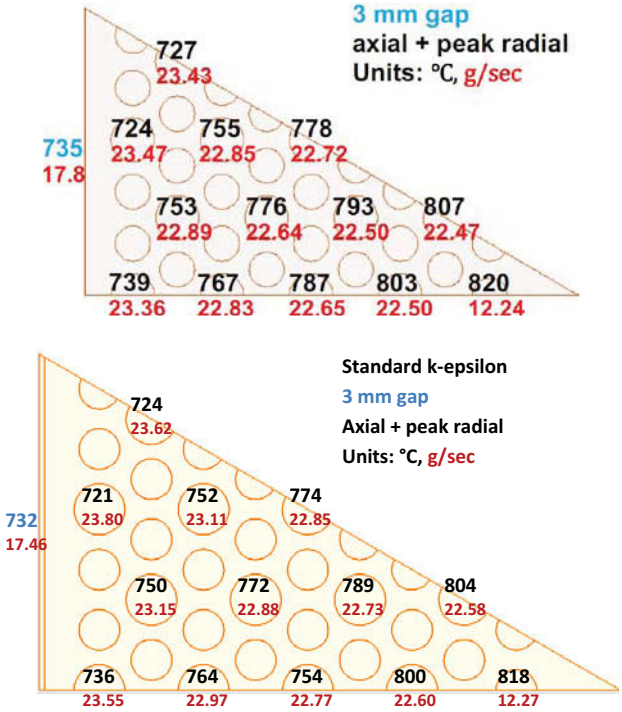

Fig. 11. Outlet temperatures and mass flow rates for FLUENT (above) and STARCCM+.

Table 3. Inputs and results for FLUENT and STARCCM+.

CFD code	FLUENT	STARCCM+
Gap width mm	3	3
Turbulence model	standard k~ε	standard k~ε 2 layer
Wall treatment	enhanced	all y^+
Inlet temperature °C	259	259
Pressure drop Pa	29900	29900
Mass flow kg/s	0.209	0.211
Gap flow fraction %	4.25	4.14
Max fuel temp °C	927	926
Gap outlet temp °C	735	732
Max channel temp °C	820	818
Max helium temp variation °C	96	97
Bulk outlet temp °C	765	762

Comparison of Turbulence Models

Results for two turbulence models using STARCCM+ are compared for the 5mm gap case for smooth graphite surfaces. The two models are the standard and realizable k~ε two layer turbulence models, both with all y+ wall treatment. For this case, the pressure drop is set to 25030 Pa in both cases; the inlet temperature is set to 259°C. The heat generation rate varies

axially at the peak radial factor (A_r = 1.25). Figure 12 plots temperature contours for the two turbulence models at the fuel hot spot, located 0.06 m above the start of the lower reflector. Though differences are apparent, the contours are very close to each other. Note the large gradient from the center to the gap.

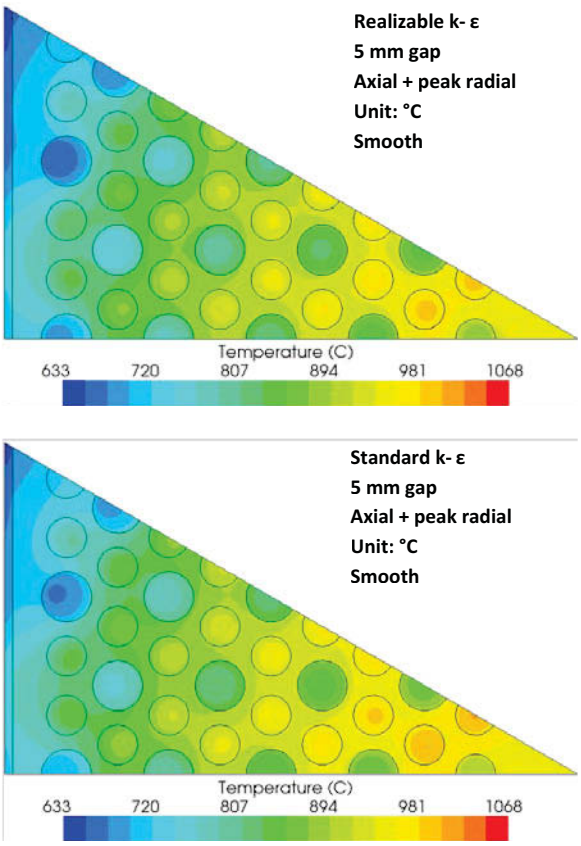

Fig. 12. Contour plots for the realizable and standard *k~ε* two layer turbulence models for 5mm gap width.

Figure 13 provides bulk outlet temperatures and helium mass flow rates for the two cases. Note that the flow rates given for the half channels are doubled to be consistent with the whole channels. The percentage differences for the two models are less than 3% based on the bulk temperature increase and the average of the two mass flows, respectively.

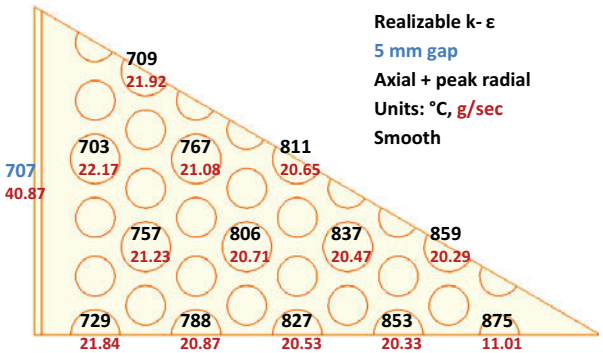

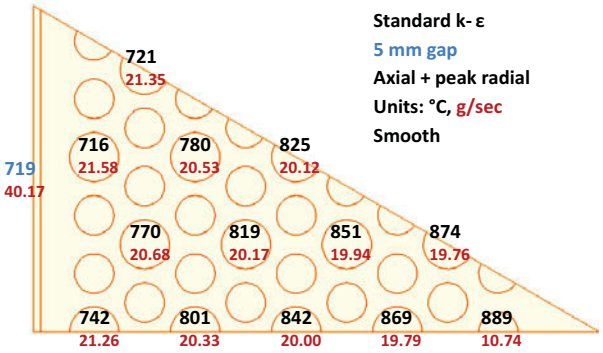

Fig. 13. Bulk outlet temperatures and mass flow rates for the two turbulence models.

Table 4 compares inputs and results for the two turbulence models. It can be seen that differences are relatively small. Note that the bulk outlet temperatures are different in order to maintain a proper heat balance because the mass flow rates are slightly different. Also note that the maximum variation in helium temperature at 172°C is significant in that this affects the amount of mixing that will be needed in the lower plenum such that the temperature of the coolant is relatively uniform as it exits the reactor vessel.

Table 4. Inputs and results for realizable and standard *k~ε* turbulence models.

Gap width mm	5	5
Turbulence model	realizable *k~ε* 2 layer	standard *k~ε* 2 layer
Inlet temperature °C	259	259
Pressure drop Pa	25030	25030
Mass flow kg/s	0.205	0.200
Gap flow fraction %	9.98	10.06
Max fuel temp °C	992	1005
Gap outlet temp °C	707	719
Max channel temp °C	875	889
Max helium temp variation °C	172	173
Bulk outlet temp °C	777	790

Effects of Surface Roughness for Various Gap Widths

In this section, the effects of two relative roughness parameters for the block graphite surfaces are examined for three gap widths: 0, 3 and 5mm widths. The surface relative roughness for flow in a tube is obtained by dividing the physical roughness height by the tube diameter. The relative roughness for the gap is obtained by dividing the roughness height by twice the gap width. In the present investigation, there are two coolant channel diameters, 15.88 and 12.70mm as well as two nonzero gap widths. In order to specify the same relative roughness for the gap and two coolant channels, the physical roughness heights have to be different for the three different coolant pathways. For all cases below, the heat generation employed is the axially varying profile at the peak radial factor (1.25) from Eqn. (1) and the inlet temperature is

259°C. For each relative roughness, the mass flow obtained using the nominal pressure drop of 29.9 kPa for zero gap width is then used for the other gap widths. This means that flow is 'stolen' from the coolant channels to flow in the bypass gap. To achieve this situation, the pressure drops in the nonzero gap width cases are reduced until the same mass flow is obtained. This allows the approximate effect of the bypass gap to be obtained, as the gap really does steal some of the flow from the coolant channels in the actual core.

Results for smooth graphite surfaces for the 350 MW_{th} HTGR using FLUENT were reported in Ref. [5]. The standard $k\sim\varepsilon$ turbulence model with the enhanced wall treatment was used therein. Inasmuch as it was shown earlier that the variations from the corresponding STARCCM+ simulations are very small, the STARCCM+ results for the smooth cases will only be summarized in table form here. The present results are computed using the realizable $k\sim\varepsilon$ two layer model using the all y^+ wall treatment, which is close to standard $k\sim\varepsilon$ results as shown above. Table 5 provides inputs and results for 0, 3 and 5mm gaps widths for smooth surfaces. The results indicate that the bypass flow more than doubles for an increase in gap width for a factor < 2. The maximum fuel temperature increases by 75°C from the zero to the 5mm gap width case. The maximum coolant temperature increases by 67°C. The greatest increase, however, is in the maximum variation in coolant temperature at the outlet from 48 to 172°C, an increase of 360%.

Table 5. Inputs and results for three gap widths for smooth graphite surfaces.

Gap width mm	0	3	5
Pressure drop Pa	29900	27770	25030
Mass flow kg/s	0.205	0.205	0.205
Gap flow fraction %	0	4.04	9.98
Max fuel temp °C	917	947	992
Gap outlet temp °C	-	748	707
Max channel temp °C	808	835	875
Max helium temp variation °C	48	99	172
Bulk outlet temp °C	777	777	777

The next three cases use a relative roughness of 0.001. The default [11] roughness equations are used such that only the actual roughness heights are specified. Again, the mass flow of the helium is found for a pressure drop of 29.9 kPa for the zero gap width case. The nonzero gap width pressure drops are then adjusted to achieve the same mass flow rate. The same axially varying heat generation at the peak radial factor is used. The realizable $k\sim\varepsilon$ two layer model with the all y^+ wall treatment is employed. Figure 14 presents the outlet temperature and mass flow rate information for the three gap width cases. The presence of the bypass gap clearly cools the block edge, creating a temperature gradient from the block center to the gap. Table 6 summarizes the inputs and results for these three cases. The surface roughness causes the mass flow to drop by 7.3% versus the smooth case, Table 5. The bypass flow percentages and variation in maximum helium temperature remain about the same versus the smooth case. The maximum fuel and coolant temperatures increase by about 40°C compared to the same gap width cases for smooth walls.

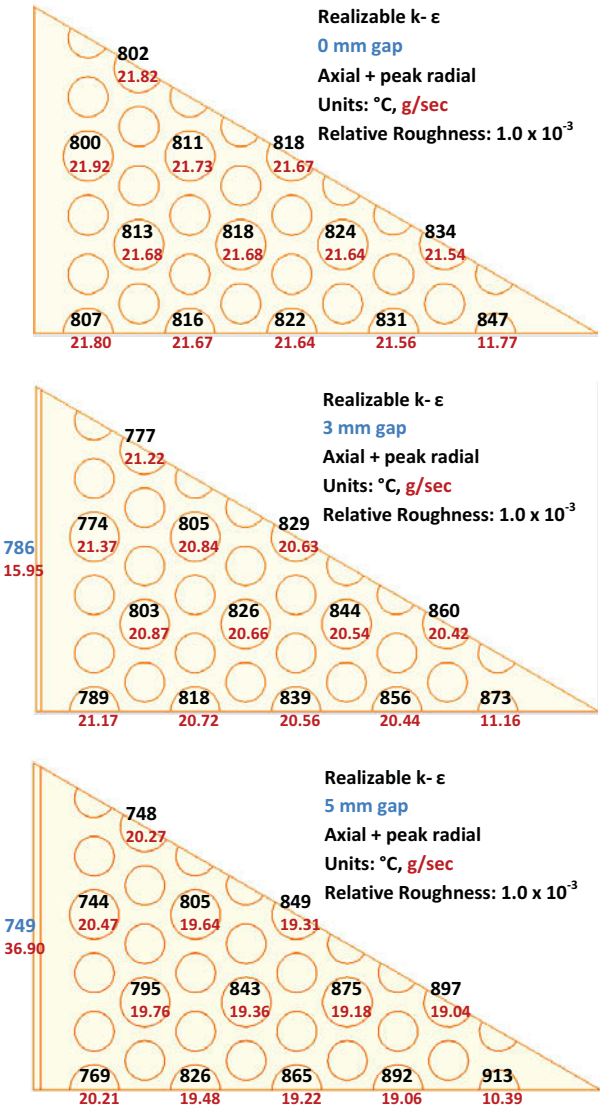

Fig. 14. Bulk outlet temperatures and mass flow rates for three gap widths for relative roughness 0.001.

Table 6. Inputs and results for three gap-widths for 0.001 relative roughness.

Gap width mm	0	3	5
Pressure drop Pa	29900	27600	24840
Mass flow kg/s	0.190	0.190	0.190
Gap flow fraction %	0	4.19	9.69
Max fuel temp °C	957	987	1030
Gap outlet temp °C	-	786	749
Max channel temp °C	847	873	913
Max helium temp variation °C	47	99	169
Bulk outlet temp °C	816	816	816

The final three cases employ a relative roughness of 0.00157. The same procedures, conditions and inputs, except for the roughness heights, are used as for the previous three cases. Figure 15 illustrates the outlet coolant temperatures and mass flow rates for the 0, 3 and 5mm gap width cases for relative roughness 0.00157. The effects of increasing gap width are again about the same as for 0.001 relative roughness. The increased roughness reduces the total mass flow by 11.7% versus the smooth wall cases. The maximum fuel and coolant temperatures are increased by about 70°C over the smooth cases. Again, the variation in maximum coolant temperature is virtually the same as for the smooth and 0.001 relative roughness cases. Table 7 shows inputs and results for these three cases.

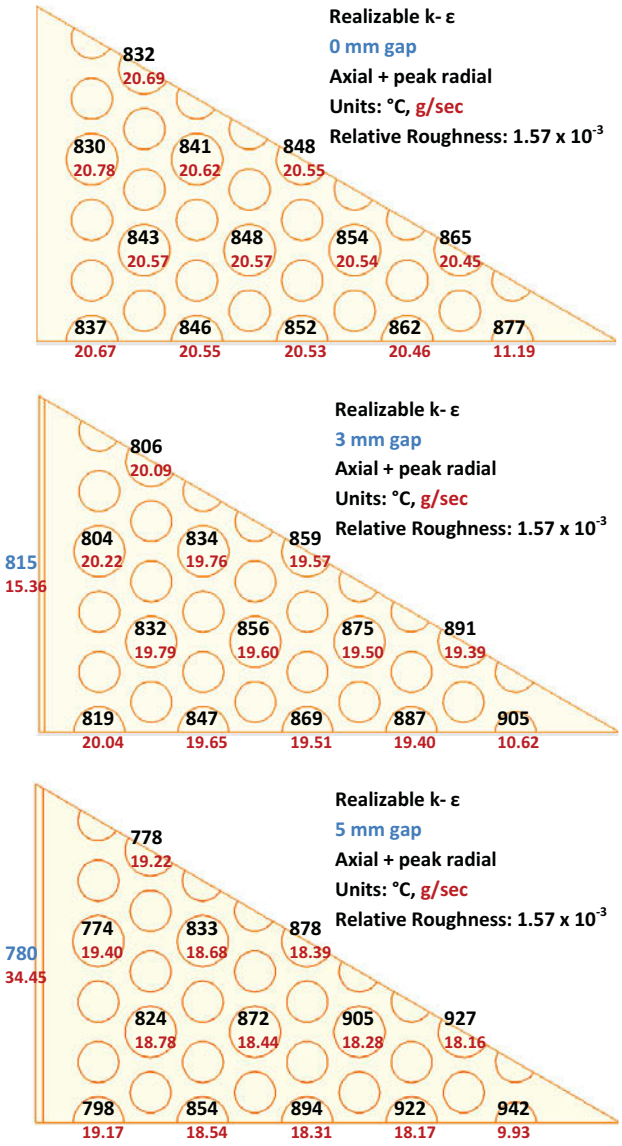

Fig. 15. Bulk outlet temperatures and mass flow rates for three gap widths for relative roughness 0.00157.

Table 7. Inputs and results for three gap-widths for 0.00157 relative roughness.

Gap width mm	0	3	5
Pressure drop Pa	29900	27500	24790
Mass flow kg/s	0.181	0.181	0.181
Gap flow fraction %	0	4.26	9.53
Max fuel temp °C	986	1018	1060
Gap outlet temp °C	-	815	780
Max channel temp °C	877	905	942
Max helium temp variation °C	47	101	168
Bulk outlet temp °C	846	846	846

SUMMARY

CFD Computations of flow in a one-twelfth sector of a prismatic HTGR block are made to compare effects of gap width and surface relative roughness. Validation exercises are performed to partially validate the calculations. However, validation data are still needed for close to actual flow conditions for full validation. Wall shear stresses, which are functions of core depth due to a changing Reynolds number, are compared to results obtained using four published friction factor correlations for eight different turbulence models. Next, the dimensionless heat transfer coefficient, the Nusselt number, is compared for four turbulence models against results obtained using a published correlation that accounts for property variation due to variation in temperature. It is noted that the correlation for Nusselt number is for smooth surfaces and may not represent values for rough surfaces. The final validation exercise is to compare wall shear stress for rough surfaces against a published correlation. It is found that the standard and realizable k~ε two layer turbulence models using the all y^+ wall treatment produce acceptable results for the validation exercises.

Employing the realizable k~ε two layer turbulence model with the all y^+ wall treatment, results are compared for smooth surfaces and two relative surface roughnesses for three gap widths. The bypass flow in the nonzero gap-width cases is 'robbed' form the coolant channel flow by lowering the pressure drop to maintain the same flow rate. The effects of gap width are found to be about the same for the three roughnesses. Increasing gap width increases the lateral temperature gradient in the block as well as the maximum fuel and coolant temperatures. The maximum variation in outlet coolant temperature dramatically increases with increasing gap width (360% for the 5mm versus the zero gap cases). The maximum coolant and fuel temperatures are further increased by about 40 and 70°C for the moderate and greater relative roughnesses, respectively.

NOMENCLATURE

AKN low Re	Abe-Kondoh-Nagano low Re turbulence model
CFD	computational fluid dynamics
D	tube diameter
DOE	U. S. Department of Energy
e	roughness (dimensional)
f	friction factor (Darcy)
HTGR	high temperature gas reactor
INL	Idaho National Laboratory, Idaho Falls, ID
k	turbulent kinetic energy
MIR	matched index of refraction facility
NGNP	next generation nuclear plant
Nu	Nusselt number (dimensionless heat transfer coefficient
Pr	Prandtl number
Re	Reynolds number
RANS	Reynolds-averaged Navier-Stokes
RKE 2 lay	Realizable k~ε two layer turbulence model
RSM 2 lay	Reynolds stress two layer turbulence model
SKE 2 lay	Standard k~ε two layer turbulence model
SKE low Re	Standard k~ε low Re turbulence model
SKΩ	Standard (Wilcox) k~ω turbulence model
SSA	Standard Spalart-Allmaras turbulence model
SST	SST (Menter) k~ω turbulence model
SST	Shear stress transport
y^+	dimensionless wall distance
ε	turbulent energy dissipation rate
ω	specific turbulent dissipation rate

ACKNOWLEDGMENTS

This manuscript has been authored by Battelle Energy Alliance, LLC under Contract No. DE-AC07-05ID14517 with the U.S. Department of Energy.

REFERENCES

[1] GA Technologies, Inc., Preliminary Safety Information Document for the Standard MHTGR, document HTGR-86-024, rev. 13, 1992.

[2] N. Tak, M-H Kim, W. Lee, Numerical investigation of a heat transfer within the prismatic fuel assembly of a very high temperature reactor, Annals of Nuclear Energy, 35, 1892-1899, 2008.

[3] H. Sato, R. W. Johnson and R. R. Schultz, "Preliminary studies of coolant by-pass flows in a prismatic very high temperature reactor using computational fluid dynamics," The 13th International Topical Meeting on Nuclear Reactor Thermal Hydraulics (NURETH-13), Kanazawa, Japan, Sept. 27 – Oct. 2 2009.

[4] H. Sato, R. W. Johnson, R. R. and Schultz, Computational Fluid Dynamic Analysis of Core By-pass Flow Phenomena in a Prismatic VHTR, *Annals of Nuclear Energy*, **37**, 1172-1185, 2010.

[5] R. W. Johnson and H. Sato, Bypass Flow Computations using a One-Twelfth Symmetric Sector for Normal Operation in a 350 MWth Prismatic VHTR, Paper 152, High Temperature Reactor 2010 Conference, Prague, The Czech Republic, October 18-20, 2010.

[6] FLUENT, ANSYS, Inc., 275 Technology Drive Canonsburg, PA 15317, 2010.

[7] http://webbook.nist.gov/chemistry/fluid/

[8] General Atomics, Safety Analysis Report use of H451 Graphite in Fort St. Vrain Fuel Elements, GLP-5588, 1977.

[9] P. MacDonald, J. Sterbentz, R. Sant, P. Bayless, R. Schultz, H. Gougar, R. Moore, A. Ougouag, W. Terry, NGNP Preliminary Point Design Results of the Initial Neutronics and Thermal-Hydraulic Assessments, INEEL/EXT-03-00870, 2003.

[10] http://journaltool.asme.org/Templates/JFENumAccuracy.pdf

[11] STARCCM+ 5.02.009, CD-adapco, 60 Broadhollow Road, Melville, NY 11747, 2010.

[12] J. A. Roberson and C. T. Crowe, *Engineering Fluid Mechanics*, 3rd ed., Houghton Mifflin Co., Boston, 1985.

[13] R. W. Fox and A. T. McDonald, *Introduction to Fluid Mechanics*, 3rd ed., John Wiley & Sons, New York, 1985.

[14] T. B. Drew, E. C. Koo and W. H.McAdams, The Friction Factor for Clean Round Pipes, Trans AICHE, 1932.

[15] D. M. McEligot, P. M. Magee and G. Leppert, Effect of large temperature gradients on convective heat transfer: The downstream region, *J. Heat Transfer*, **87**, 67-76, 1965.

[16] C. Warburton, Surface Roughness of Graphite and its Effect on Friction Factor, *Proc. Instn. Mech. Engrs*., **188**, 457-460, 1974.

[17] J. Nikuradse, Strömungsgesetze in rauhen rohren, *Trans. NACA* TM 1292, 1933.